D301.45/33-3:61-63

AEDC-TN-61-63

T. PAUL TORDA

A FORCED-OSCILLATION BALANCE SYSTEM FOR THE von KÁRMÁN FACILITY 40- BY 40-INCH SUPERSONIC TUNNEL

By

C. J. Welsh, Q. P. Hance, and L. K. Ward
VKF, ARO, Inc.

May 1961

ARNOLD ENGINEERING DEVELOPMENT CENTER

AIR FORCE SYSTEMS COMMAND

U S A F

ILLINOIS INSTITUTE OF TECHNOLOGY
IIT LIBRARY
JUL 1 3 1962
GOVERNMENT PUBLICATIONS
DEPOSITORY 0040-A

Additional copies of this report may be obtained from

ASTIA (TISVV)
ARLINGTON HALL STATION
ARLINGTON 12, VIRGINIA

note

Department of Defense contractors must be established for ASTIA services, or have their need-to-know certified by the cognizant military agency of their project or contract.

A FORCED-OSCILLATION BALANCE SYSTEM FOR THE von KÁRMÁN FACILITY 40- BY 40-INCH SUPERSONIC TUNNEL

By

C. J. Welsh, Q. P. Hance, and L. K. Ward
VKF, ARO, Inc.

May 1961

ARO Project No. 330056
Program Area 750A, Project 8952

Contract No. AF 40(600)-800 S/A 11(60-110)

AF - AEDC
Arnold AFB Tenn

ABSTRACT

A description of a recently developed, forced-oscillation balance system for the von Kármán Gas Dynamics Facility's 40- by 40-inch supersonic wind tunnel is given. Measured damping-in-pitch derivatives for a flared afterbody re-entry shape at $M_\infty = 4$ over a Reynolds number range from 0.37×10^6 to 0.58×10^6 based on body diameter are presented.

CONTENTS

	Page
ABSTRACT	3
NOMENCLATURE	6
INTRODUCTION	7
APPARATUS	
Wind Tunnel	7
Dynamic Balance System	7
Model	9
PROCEDURE	9
PRECISION OF MEASUREMENT	10
RESULTS AND DISCUSSION	11
CONCLUDING REMARKS	12
REFERENCES	12

ILLUSTRATIONS

Figure		
1.	Tunnel A, a 40- by 40-in. Supersonic Wind Tunnel	13
2.	Sting Balance Assembly of the Forced-Oscillation Balance System	14
3.	Assembly View of the Balance System and Model	15
4.	Forward End of the Small Amplitude Forced-Oscillation Balance	16
5.	Diagram of Control and Data Recording System	17
6.	Model Configuration	18
7.	Damping-in-Pitch Derivatives for a Flared Afterbody Configuration at $M_\infty = 4$	19

NOMENCLATURE

C_{m_q} $C_{m_{\dot{\alpha}}}$	$C_{m_{(qd/2V_\infty)}}$ $C_{m_{(\dot{\alpha}d/2V_\infty)}}$ } Damping derivatives, 1/radian
d	Model diameter, ft
I	Moment of inertia, slug-ft^2
M_∞	Free-stream Mach number
M_θ	Angular restoring-moment parameter, ft-lb/radian
$M_{\dot{\theta}}$	Angular viscous-damping parameter, ft-lb-sec/radian
$M'_{(\dot{\theta}/\omega)}$	Aerodynamic damping parameter, ft-lb/radian = $M_{(\dot{\theta}/\omega)_{\text{wind-on}}} - M_{(\dot{\theta}/\omega)_{\text{vacuum}}}$
q	Angular velocity, radian/sec
q_∞	Free-stream dynamic pressure, lb/ft^2
Re	Reynolds number, based on basic body diameter
S	Model cross section area (basic body diameter), ft^2
T	Input torque function, ft-lb
V_∞	Free-stream velocity, ft/sec
α	Angle of attack, radian
$\dot{\alpha}$	Time rate of change of angle of attack, radian/sec
θ	Angular displacement, radian
$\dot{\theta}$	Angular velocity, radian/sec
$\ddot{\theta}$	Angular acceleration, radian/sec^2
ω	Angular frequency, radian/sec

SUBSCRIPT

o	Maximum values

INTRODUCTION

A dynamic balance system has been developed for the 40- by 40-in. supersonic tunnel (Tunnel A) of the von Kármán Gas Dynamics Facility (VKF), Arnold Engineering Development Center. This balance is a forced-oscillation system, having one degree of freedom in rotation about a fixed-pivot axis, which permits measuring damping derivatives in pitch or yaw. The system is equipped with a velocity feedback, amplitude control system permitting tests of configurations that are either dynamically stable or unstable.

Results of tunnel evaluation tests of this balance including damping-in-pitch derivatives measured on a flared afterbody re-entry configuration at $M_\infty = 4$ are presented.

APPARATUS

WIND TUNNEL

Tunnel A (Fig. 1) is a 40- by 40-inch, continuous, closed circuit, variable-density, supersonic wind tunnel with a Mach number range from 1.5 to 6. The top and bottom walls of the nozzle are flexible plates which are automatically positioned at the desired contours by electrically driven screw jacks. The tunnel is driven by a 100,000- horsepower compressor system which provides maximum tunnel stagnation pressures of 2 to 13.5 atmospheres at $M_\infty = 1.5$ and $M_\infty = 6$, respectively. Minimum operating pressures are less than one tenth of the maximum. A complete description of the tunnel may be found in Ref. 1.

DYNAMIC BALANCE SYSTEM

The dynamic balance (Fig. 2) is a sting supported, cross-flexure pivot system permitting one degree-of-freedom angular motion with an oscillation amplitude up to approximately ±2 deg. The forward end of the pivot system to which the model is attached is forced to oscillate through a linkage by an electro-magnetic shaker housed in the enlarged portion of the sting. The model (Fig. 3) can be secured during the starting and the stopping of the tunnel with a solenoid-actuated locking device shown in Fig. 4. The use of sets of cross flexures having different stiffness values provide additional flexibility in testing over a frequency range.

Manuscript released by authors May 1961.

The motion of such a simple forced system can be defined by the equation

$$I\ddot{\theta} - M_{\dot{\theta}}\dot{\theta} - M_{\theta}\theta = T \qquad (1)$$

It can be shown from Eq. (1) that, as the model is oscillated at a constant amplitude and at the undamped natural frequency of the system, the inertia moment exactly balances the restoring moment, and that the torque required is exactly equal to the damping moment.

To provide amplitude control, the balance system has been equipped with an electronic feedback control circuit. Instrumentation and control circuitry are shown in block diagram in Fig. 5. Resistance strain gages, bonded to the input torque member and to one of the cross-flexure pivot members of the model support structure, were arranged electrically as bridges and served as input transducers supplying torque and displacement signals to the 20-kc carrier amplifier. The two output signals of the carrier amplifier operated the galvanometers of a direct-writing oscillograph and provided recorded traces of the torque and displacement signals. The galvanometers provided response which was flat within ±0.25 percent over the range of frequencies of the recorded data. A 60-cps signal was also recorded on the oscillograph and served as a time base from which frequency data could be determined.

In addition to providing a recorded amplitude trace, the displacement signal output from the carrier amplifier also served as an input to the electronic amplitude control system. The amplitude controller is a true feedback system in which the model displacement signal is compared with a reference signal, and the amplified difference signal is used to drive the shaker motor. Any change in the amplitude of the displacement signal will produce an inverse change in the driving signal and will thus tend to hold the displacement signal constant at a level determined by the level of the reference signal. The frequency of oscillation is controlled by the reference oscillator and can be set to the natural resonant frequency of the balance system. A shaker motor, driven by a 250-watt d-c power amplifier, provided the torque necessary to sustain the resonant, sinusoidal motion of the model. An oscilloscope displaying a Lissajous pattern of the torque versus displacement signals served to indicate the 90-deg phase angle between these two signals necessary to the condition of resonance.

The operation of the closed-loop, feedback amplitude controller is similar to that of a basic servo operating on the amplified error principle. The reference signal is supplied by a built-in, highly stable, low distortion, feedback oscillator. The displacement signal is phase shifted approximately 90 deg by an electronic phase shift network so that it is

in phase with the reference signal. The two signals are then compared in a difference amplifier, and the difference or error signal is amplified and used to drive the shaker motor. The error signal will remain in phase with the reference signal for all conditions requiring a positive application of torque to sustain the model oscillations.

The phase shift network is ganged with the frequency control of the reference oscillator so that when the correct phase shift has been set in, it will remain correct even though the frequency is changed. The loop or amplifier gain determines the rate of response of amplitude control, that is, the amount of restoring torque applied for a given change in displacement signal. Once the rate of control has been set, the frequency and amplitude of oscillations are controlled by the reference oscillator. The frequency range of the present system is from 2 to 60 cycles per second. This control system will, without any change in setup, control the amplitude of the model oscillations in the region of aerodynamic instability.

In view of amplitude control considerations, it is advantageous to operate a forced-oscillation balance at a frequency displaced from the natural frequency of the system under certain test conditions. Effort is currently being directed to provide the system with a resolving network to permit determining the in-phase and out-of-phase components of the forcing vector, and in turn the damping of the system when operating at a non-resonant frequency.

Though the balance system has been designed for the 40 by 40-in. supersonic tunnel, the system can be used equally as well in the 50-in. hypersonic tunnels (Tunnels B and C) with the addition of water cooling and air jets to permit cooling of the balance.

MODEL

A sketch of the model configuration is shown in Fig. 6. The model was constructed of laminated Fiberglas with aluminum bulkheads, and ballast was distributed to place the model's center of gravity at the pivot axis. The basic body diameter (d) was five inches.

PROCEDURE

In the present test damping data were obtained at the undamped natural frequency of the model-balance system; hence, the required forcing torque is precisely equal to the damping torque of the system

for constant amplitude motion. The method for computing the dimensionless damping derivatives from the constant amplitude forced-oscillation tests is indicated by the following expressions:

$$M_{\dot{\theta}\dot{\theta}} = T \text{ (at the undamped natural frequency of the system)}$$

$$M_{\dot{\theta}\theta_o\omega} = T_o$$

$$M(\dot{\theta}/\omega) = T_o/\theta_o$$

$$M'(\dot{\theta}/\omega) = M(\dot{\theta}/\omega)_{\text{wind on}} - M(\dot{\theta}/\omega)_{\text{vacuum}}$$

$$C_{m_q} + C_{m_{\dot{\alpha}}} = 2V_\infty M'(\dot{\theta}/\omega)/q_\infty S d^2 \omega$$

The expression for obtaining the aerodynamic parameter $M'_{(\dot{\theta}/\omega)}$ follows from the premise that the structural damping of a flexure pivot varies inversely with the frequency of oscillation (Ref. 2).

Tests of the flare model were made at $M_\infty = 4$ and over a Reynolds number range (based on body diameter) from 0.37×10^6 to 0.58×10^6. The amplitude of model oscillation was approximately ±1.5 deg, and measurements were made over an angle-of-attack range from 0 to 14.5 deg. The range of model frequency varied from 10.8 to 12 cps, and measurements were made for a pivot axis location of 43 and 56 percent of the model body length.

A thin circular metal disk that could be positioned at the juncture of the removable model nose was used for the addition of nose roughness to the model. The portion of the disk extending past the model surface (approximately one-eighth inch) had triangular sections removed leaving a series of triangles surrounding the nose of the model.

The balance was equipped with removable sting tie-rods for increasing the stiffness of the support system; however, no appreciable effects on the damping were measured.

PRECISION OF MEASUREMENT

The balance was calibrated statically during bench tests. By use of known displacements and moments, transducer calibration factors were obtained for the model displacement and the input torque. Resulting

errors in either parameter were within ±0.75 percent of the maximum value of the range in which each parameter was calibrated. Identical instrumentation cabling was used during the tunnel tests and during calibration; errors attributed directly to instrumentation are estimated to be within ±0.5 percent. Errors in determining ω values from recorded traces were within ±0.5 percent, and the error in the $(V/q)_\infty$ parameter also used in reducing the data had an estimated uncertainty of ±1.0 percent.

The displacement and torque signals were monitored continuously on the oscilloscope during testing, and errors of an electrical or mechanical nature that would result in a distorted, sinusoidal, model motion were immediately apparent. The aerodynamic damping was obtained as the difference between that for a wind-off vacuum condition (structural damping of the cross-flexure pivot system) and the total damping measured during wind-on conditions.

Considering the uncertainties in the above individual measurements and the fact that the aerodynamic damping parameter is determined as a function of the difference in wind-on conditions and tare values, an estimated maximum uncertainty of ±1.5 in $C_{m_q} + C_{m_{\dot{\alpha}}}$ values was obtained.

RESULTS AND DISCUSSION

The forced-oscillation balance was satisfactorily operated as both a positive and a negative damped system and over a range of operating conditions.

Damping-in-pitch data measured at $M_\infty = 4$ and representative of the more extreme operating conditions are presented in Fig. 7 for the flared afterbody re-entry shape to demonstrate the balance capability for testing over a range of angle of attack and of dynamically unstable configurations. Damping values measured at Reynolds numbers of approximately 0.37×10^6 and 0.58×10^6, based on body diameter, indicated that the damping of the flared configuration with nose roughness increased with angle of attack. As has been previously observed, some flared shapes in this Mach number range are dynamically unstable without nose roughness; hence, by removing the nose roughness disk the system could be operated in an unstable region. As indicated in Fig. 7 the flared shape had an appreciable amount of instability in this condition; however, amplitude control of the model could be maintained equally as well as in the stable region.

CONCLUDING REMARKS

Damping-in-pitch derivatives measured at $M_\infty = 4$ indicate that the balance system can be used satisfactorily for damping tests including measurements at angles of attack and for dynamically unstable models.

REFERENCES

1. Schueler, C. J. and Strike, W. T. "Calibration of a 40-Inch Continuous Flow Tunnel at Mach Numbers 1.5 to 6." AEDC-TN-59-136, November 1959.

2. Welsh, C. J. and Ward, L.K. "Structural Damping in Dynamic Stability Testing." AEDC-TR-59-5, February 1959.

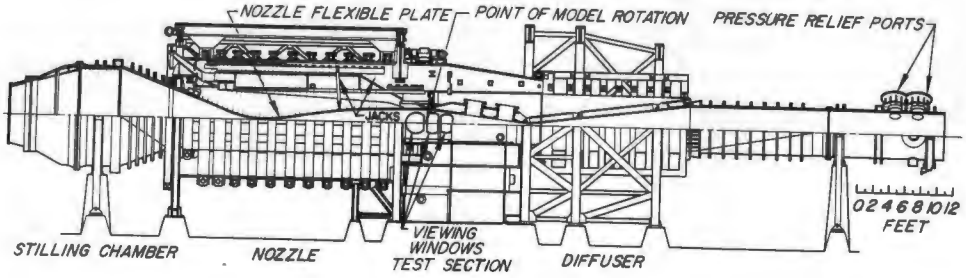

Assembly

Nozzle and Test Section

Fig. 1 Tunnel A, a 40 by 40-in. Supersonic Wind Tunnel

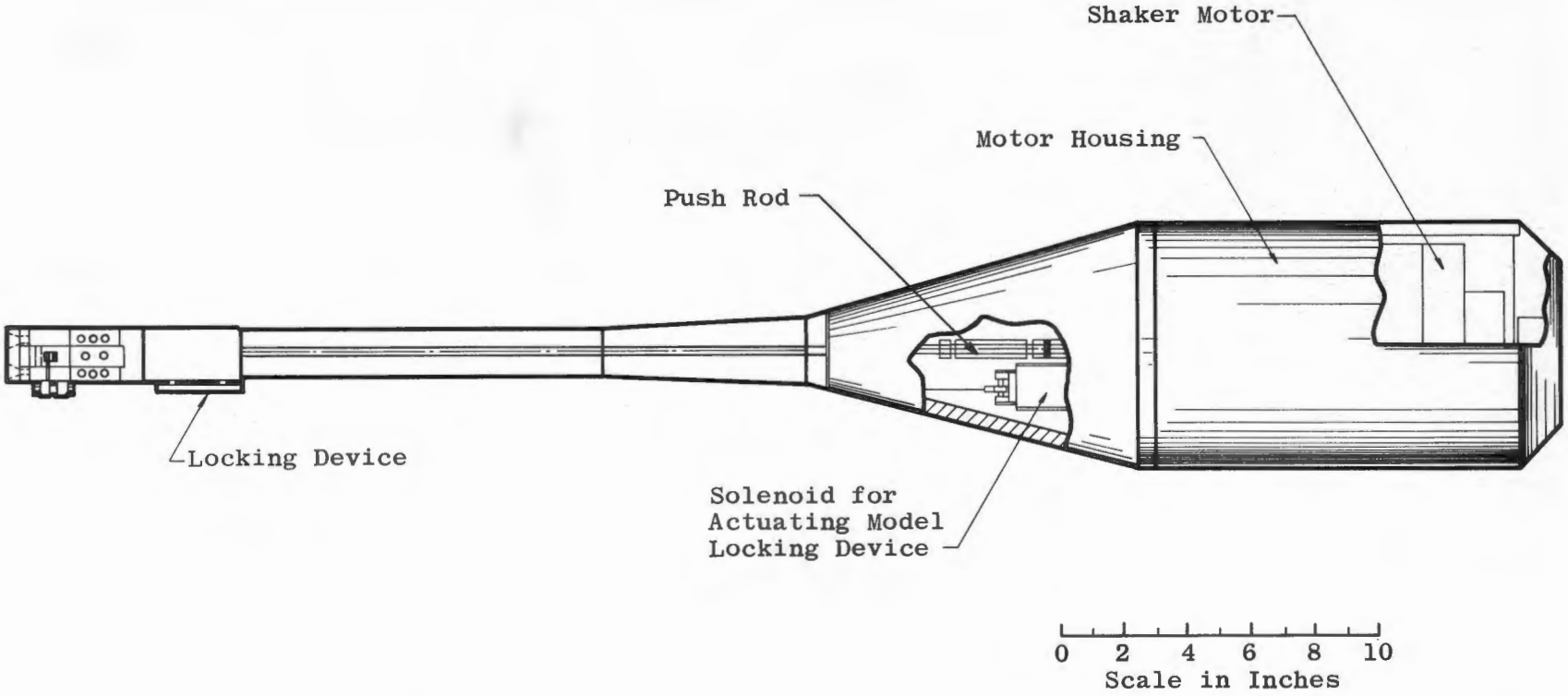

Fig. 2 Sting Balance Assembly of the Forced-Oscillation Balance System

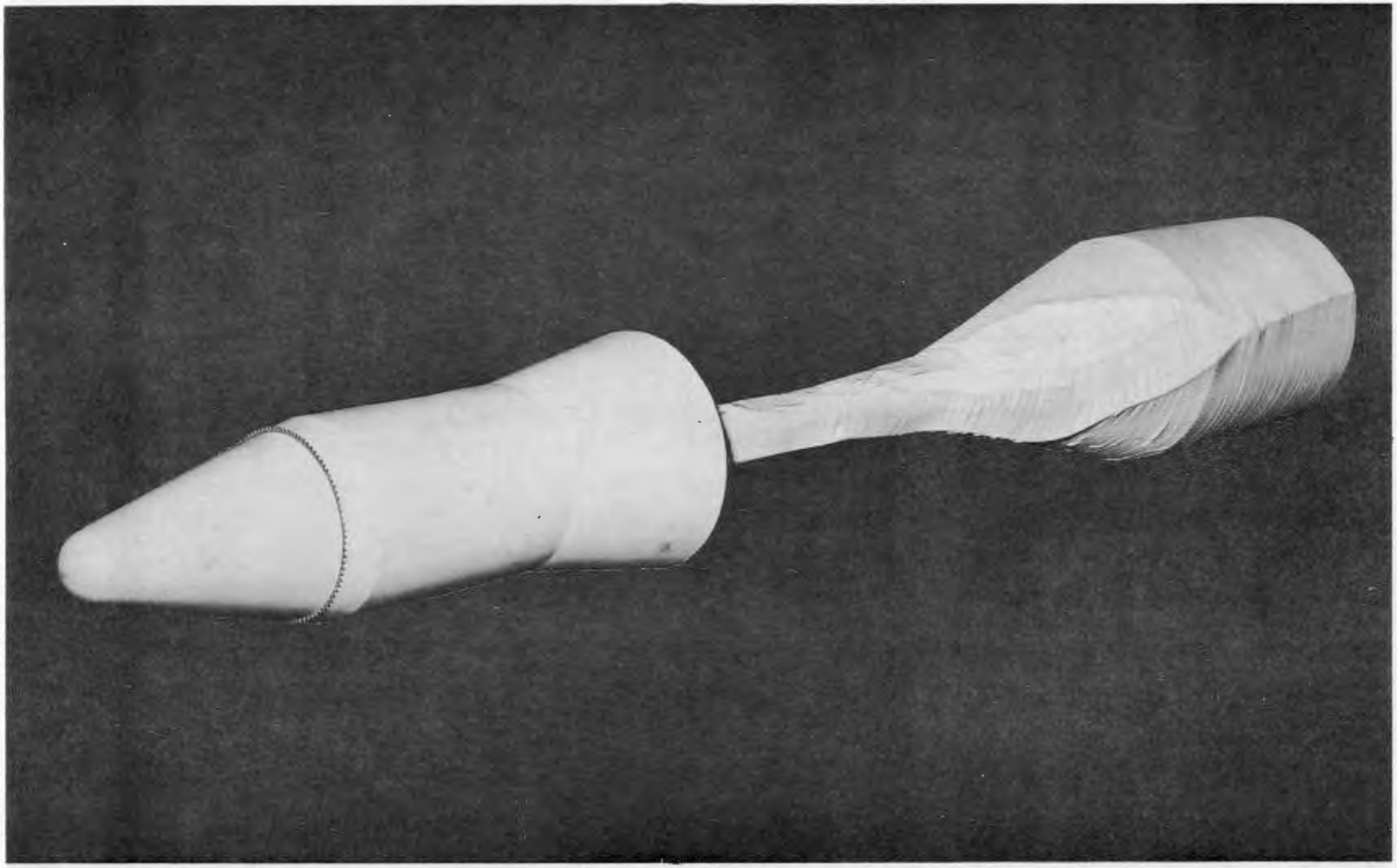

Fig. 3 Assembly View of the Balance System and Model

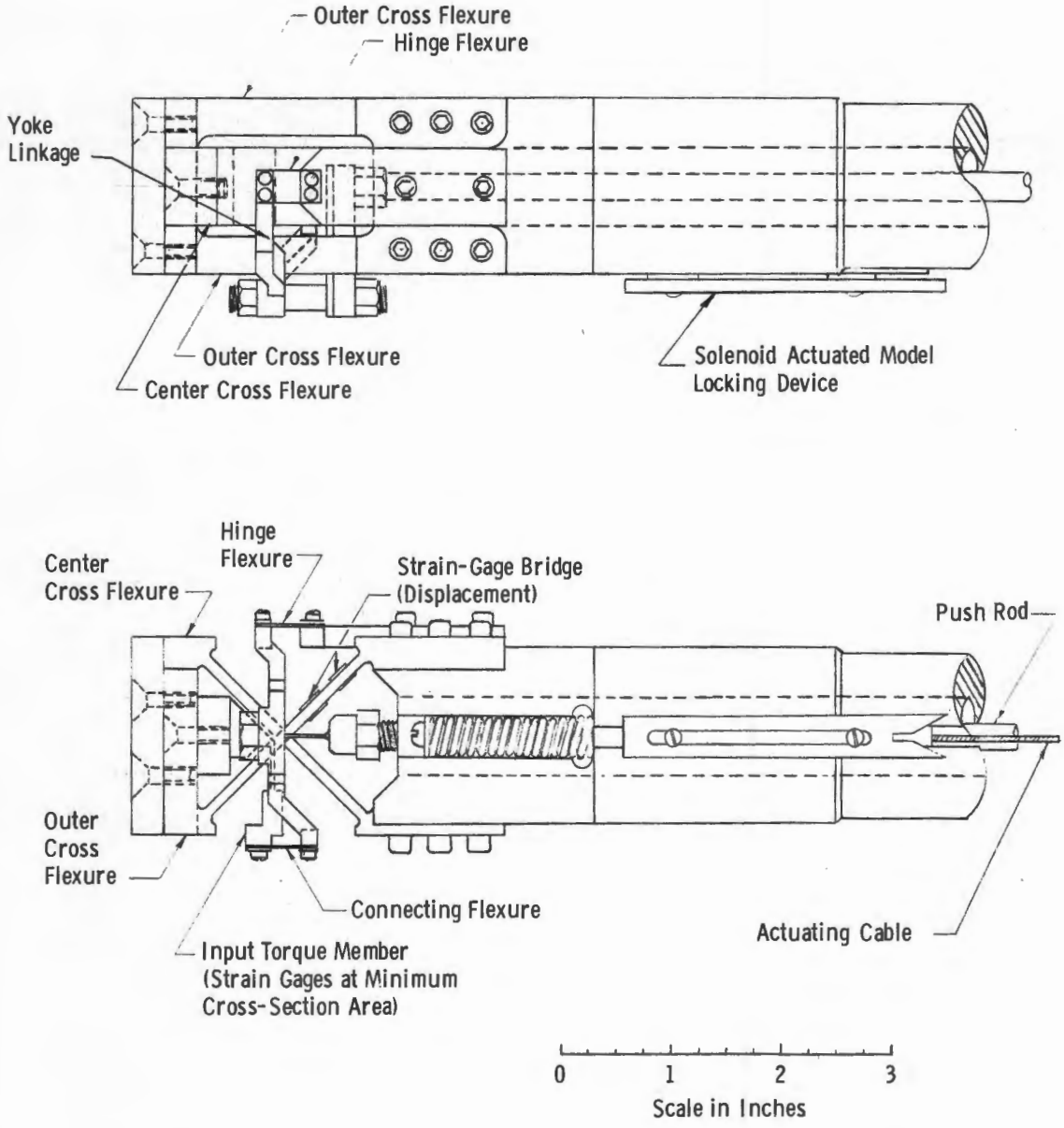

Fig. 4 Forward End of the Small Amplitude Forced-Oscillation Balance

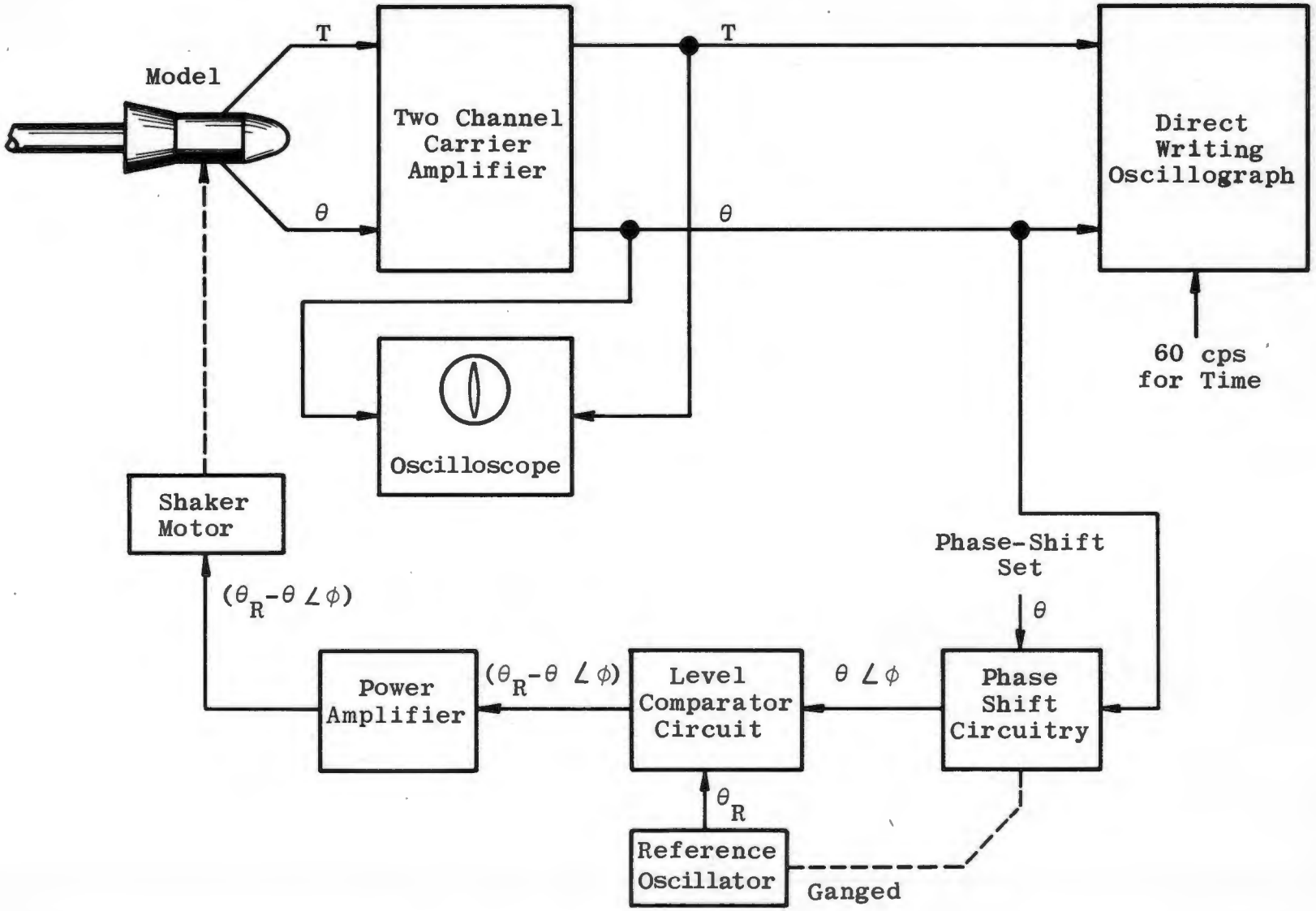

Fig. 5 Diagram of Control and Data Recording System

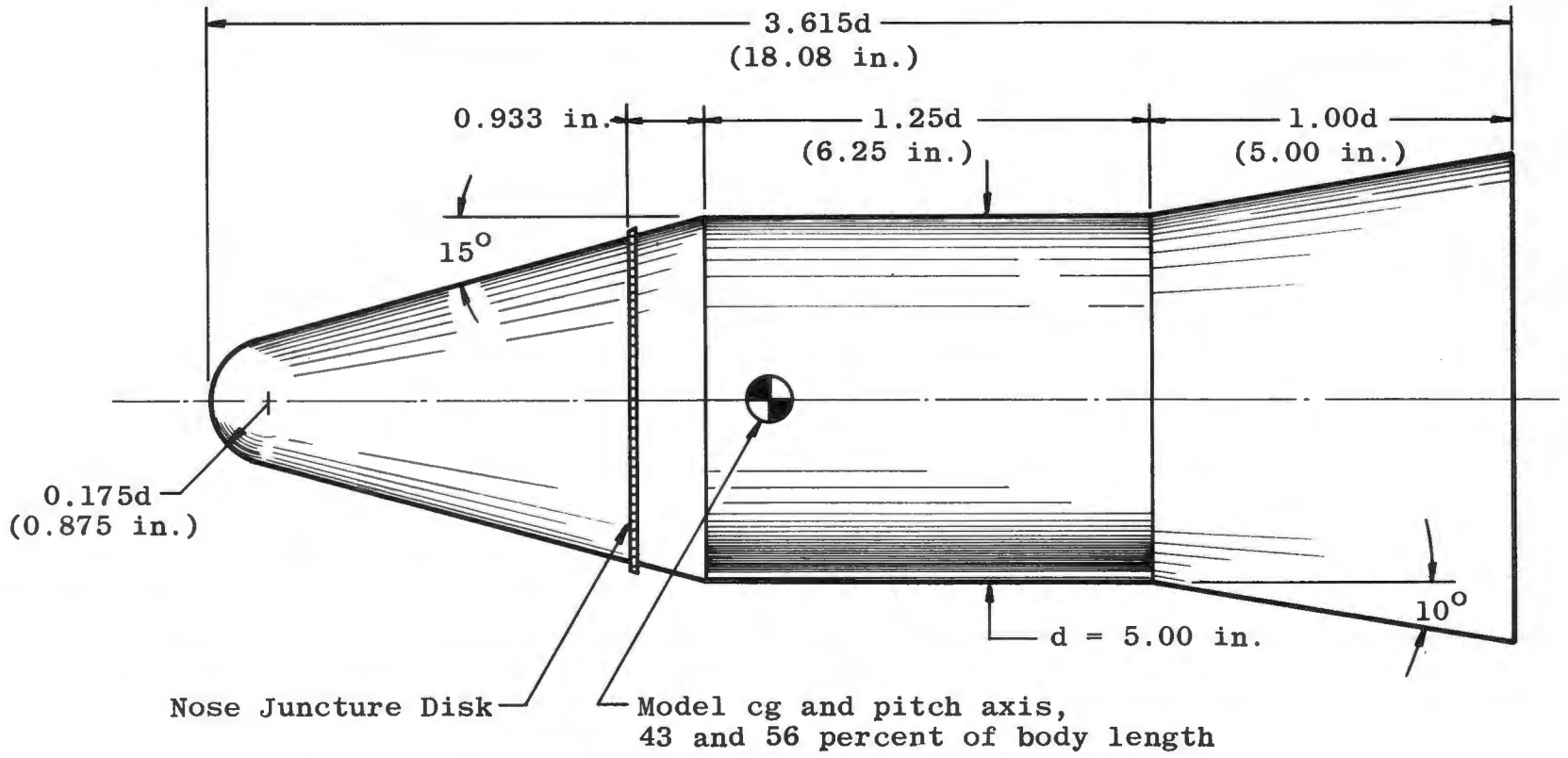

Fig. 6 Model Configuration

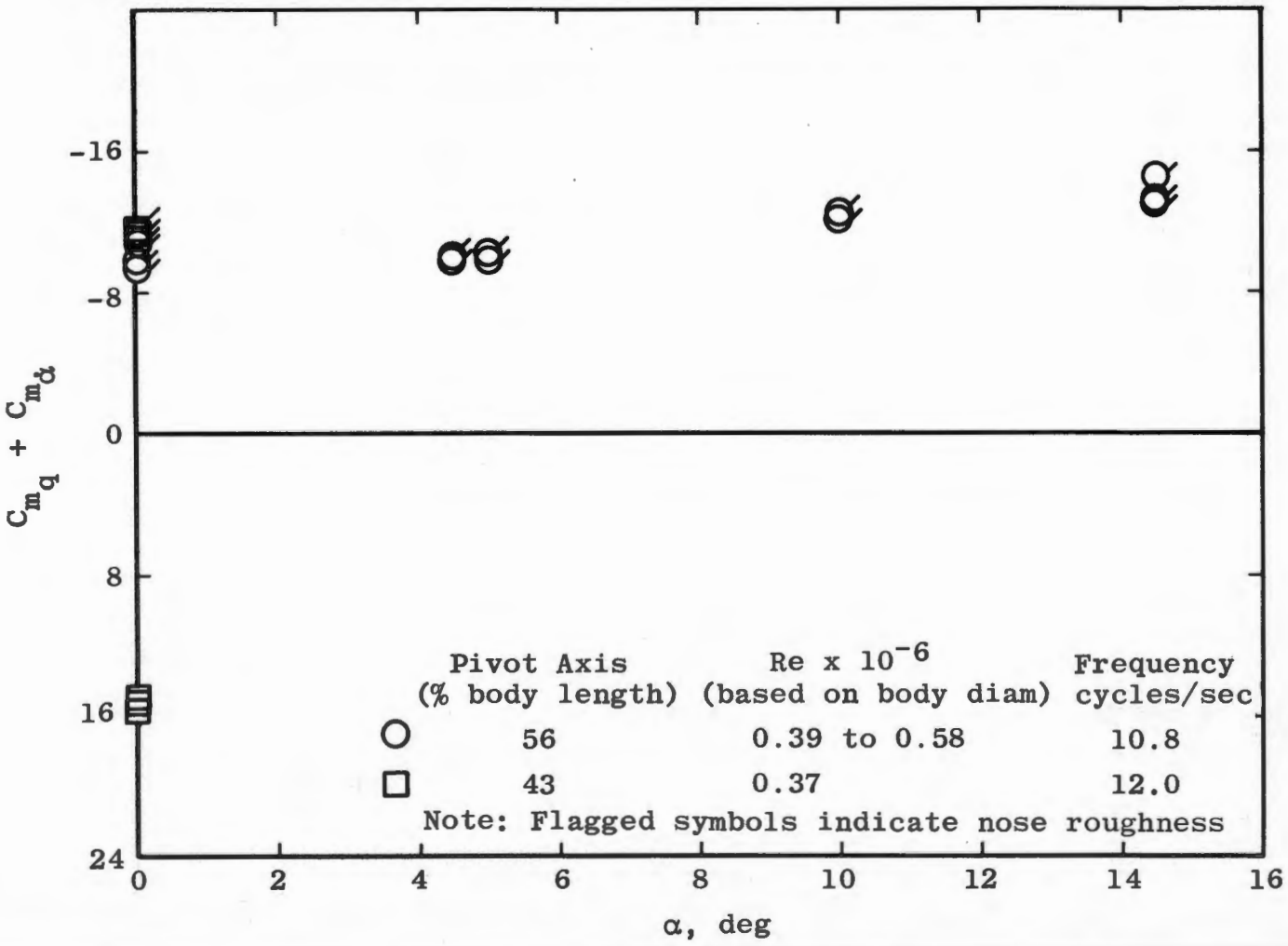

Fig. 7 Damping-in-Pitch Derivatives for a Flared Afterbody Configuration at $M_\infty = 4$